

# Mechanical deformation of high-purity sputter-deposited nano-twinned copper

A.M. Hodge,<sup>a,\*</sup> Y.M. Wang<sup>b,c</sup> and T.W. Barbee, Jr.<sup>b,c</sup>

<sup>a</sup>*Aerospace and Mechanical Engineering Department, University of Southern California, Los Angeles, CA 90089-1453, USA*

<sup>b</sup>*Materials Science and Technology Division, Lawrence Livermore National Laboratory, Livermore, CA 94550, USA*

<sup>c</sup>*Nanoscale Synthesis and Characterization Laboratory, Lawrence Livermore National Laboratory, Livermore, CA 94550, USA*

Received 12 November 2007; revised 25 February 2008; accepted 28 February 2008

Available online 10 March 2008

Near classical yield points were reproducibly observed at room and liquid nitrogen temperatures during tensile deformation of 170  $\mu\text{m}$  thick, high-purity copper foils synthesized by magnetron sputter deposition. Uniformly distributed mobile dislocations introduced by rolling to  $\sim 20\%$  reduction in thickness eliminated the yield point at both temperatures. The experimental observations clearly demonstrate that the observed yield-point behavior is a direct result of the very low initial dislocation density in these sputtered films as expected for “ideal” nanoscale microstructural materials.

© 2008 Acta Materialia Inc. Published by Elsevier Ltd. All rights reserved.

**Keywords:** Yield point; Nano-twinned; Sputtering; Multilayer thin films

Yield-point drops are a classic non-uniform plastic deformation process in solids. The dependence of the yield-point-drop phenomenon in crystalline solids has been clearly related to the availability of necessary mobile dislocations to support the plastic deformation process, as elucidated by Johnston and Gilman [1] in their classic work on single crystal lithium fluoride. This deformation process was subsequently demonstrated to result in yield point behavior for a broad range of solids, including the body-centered cubic (bcc) transition metals.

In this paper we consistently use the term “ideal” to describe a nano materials state important to the mechanical properties. This structural state is one that is expected from theory and model calculations yet unobserved in real materials presented in prior work. Ideal nanostructured materials, characterized by a high density of interfaces and nearly defect-free grain interiors [2] and a lack of the necessary mobile dislocations to support the plastic deformation. Thus, one may expect to see the yield peaks in these nanostructured materials; however, yield peak behavior has not been observed experimentally [3–6]. Molecular dynamics (MD) simulations of dislocation-free nanocrystalline

microstructures have indeed demonstrated that the deformation regime is characterized by yield-point phenomena, but this could be due to the ultrahigh strain rates used in MD simulations [7]. Yu et al. [8] recently reported the yield peak behavior in ultra-fine-grained (UFG) aluminum alloys ( $\sim 350$ – $450$  nm), which may be attributed to the pinning of mobile dislocations by solute atoms. The conclusive evidence on the yield peaks of pure nanostructured materials has not yet been forthcoming.

In this letter, we present the reproducible observations of yield peaks in high-purity nanostructured Cu with mediate-density growth twins, as a direct result of the low initial dislocation density and nanoscale twin spacing ( $\sim 45$ – $50$  nm). Previous publications regarding UFG copper with nanoscale twins (produced by electro-deposition) have shown an increase in strength and ductility related to the twin density [9–12]; however, there has been no observation of a yield peak behavior. We will discuss the origin of such discrepancies in these materials.

High-purity (99.99%+) Cu/Cu foils 170  $\mu\text{m}$  thick with individual deposition layer thickness of 2.5 nm were deposited onto 10 cm diameter (100) silicon wafers by d.c. magnetron sputtering, following the procedures described in a previous publication [13–16]. It is important to note that the films were “freely” removed from the substrate and were handled as free-standing foils

\* Corresponding author. Tel.: +1 213 740 4225; fax: +1 213 740 8071; e-mail: [ahodge@usc.edu](mailto:ahodge@usc.edu)

after deposition. Specifically, the 25  $\mu\text{m}$  thick samples from our previous study were peeled off from the silicon substrate, and therefore easily deformed; however, in this study the samples are  $\sim 170 \mu\text{m}$  thick. According to the Euler–Bernoulli beam theory (the film stiffness  $k \propto t^3$ , where  $t$  is the thickness), the 170  $\mu\text{m}$  thick samples are  $\sim 500$  times stiffer than the thinner films, which prevents deformation during their removal from the substrate. The increase in stiffness allows us to handle the sample without introducing deformation and thus maintain a relatively low dislocation density in the material.

Characterization of the as-deposited samples was performed by using both SEM analysis of etched surfaces and by using a Philips CM300-FEG transmission electron microscope (TEM) at 300 kV. Plan-view TEM samples were thinned to transparency using an E.A. Fischione (PA, USA) twin-jet electropolisher in an electrolytic solution of 10 vol.% nitric acid and 90% methanol at a temperature of  $-25^\circ\text{C}$ . The cross-sectional TEM samples were prepared using a dual-focused ion beam (FIB) technique. Figure 1a is a representative plan-view TEM image reflecting the low dislocation structure of the as-prepared film, whereas Figure 1b shows a plan-view TEM image of the 20%-rolled Cu foil sample at RT. Heavily tangled dislocations are evident. Figure 1c shows a cross-sectional TEM micrograph of the as-prepared sample with nanoscale twins (40–80 nm lamella spacing). Note that the twin boundaries are perpendicular to the growth direction; approximately 95% of the grains (columnar grain diameter 500–600 nm) have extensive nanoscale twinning with an average twin density  $\geq 3 \times 10^6 \text{ m}^2 \text{ m}^{-3}$ . Overall, the microstructure shows columnar grains as reported in our previous publication [16].

Given the importance of maintaining a low dislocation density material, all tensile samples were cut from a die at room temperature in order to prevent grain growth and possible damage from machining process. A special mounting fixture was also designed to minimize handling of the samples and prevent any damage or bending during tensile test setup. Tensile tests were performed at room and liquid nitrogen temperature

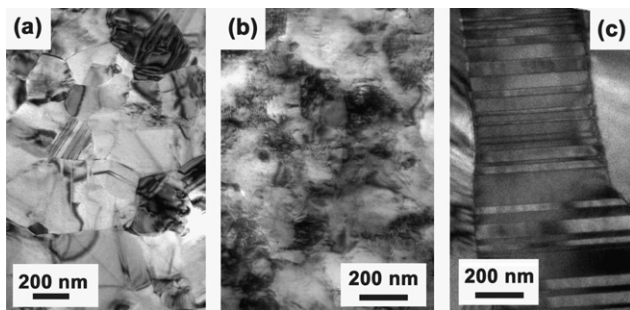


**Figure 1.** Representative TEM micrographs of the film in (a) plan-view reflecting the low dislocation structure of the film and (b) plan-view TEM image of the 20%-rolled Cu sample at RT. Heavily tangled dislocations are evident (c) cross-section noting the nanoscale twins (40–80 nm lamella spacing). Note that the twin boundaries are perpendicular to the growth direction; approximately 95% of the grains.

using an Instron 4444 table-top universal testing machine and dogbone-shaped samples with 6 mm gauge length, 3 mm width, and thickness of 170  $\mu\text{m}$ . Strain rates vary from  $10^{-5}$  to  $10^{-2} \text{ s}^{-1}$ . Tests in liquid nitrogen were held in a container attached to a condenser to maintain a steady temperature. Strain was calculated from cross-head displacement after subtraction of the machine compliance. A laser extensometer was used in all RT tests. Figure 2 shows representative RT stress–strain curves at three different strain rates. From these results one can calculate a strain rate sensitivity,  $m = 0.021$ , by using equation  $m = \frac{\partial \ln \sigma}{\partial \ln \dot{\epsilon}}$ . This result is consistent with findings by Dao et al. [11] on medium twin density Cu ( $m \sim 0.026$ ) samples prepared by electrodeposition.

The observed yield peaks in Figure 2 are reproducible and are apparently insensitive to the deformation strain rates. We suggest that this phenomenon is related to the nanoscale twins which pin the dislocations and create a shortage of mobile dislocations. Specifically, using the Orowan equation, the plastic strain rate of a material is given by  $\dot{\epsilon} = bnv$ , where  $b$  is the burgers vector,  $n$  is the number of dislocations per unit area, and  $v$  is the average dislocation velocity. Thus, in a material where  $n$  is very small, the higher stress is required to nucleate or initiate mobile dislocations which could be pinned by the presence of evenly distributed dislocation barriers (i.e. grain boundaries, interstitials). A subsequent lower stress level is required to move these mobile dislocations once they escape from the pinning area, leading to yield peaks as shown in Figure 2.

Thus far, we have emphasized the high purity and the low initial dislocation density of the material with reproducible yield peak results. In order to verify the effect of the initial dislocation density on the yield behavior, we introduce dislocations by room-temperature rolling. The as-synthesized foils were rolled to  $\sim 22\%$  thickness reduction and then cut into dogbone samples for tensile testing. Figure 3 incorporates a comparison of typical stress–strain curves at a given strain rate ( $1 \times 10^{-3} \text{ s}^{-1}$ ) for tensile tests performed for as-synthesized and rolled material at RT (Fig. 3a) and 77 K (Fig. 3b), respectively. The large deformation from the rolling process induces internal dislocations (see Fig. 1b) that allow the material

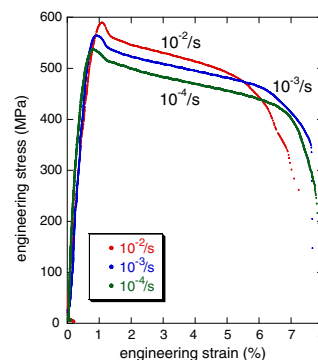


**Figure 2.** Engineering stress–strain curves for foils tensile tests performed at room temperature at various strain rates ( $10^{-2} \text{ s}^{-1}$ ,  $10^{-3} \text{ s}^{-1}$ ,  $10^{-4} \text{ s}^{-1}$ ). Note that yield peaks are reproducible and insensitive to the deformation strain rates.

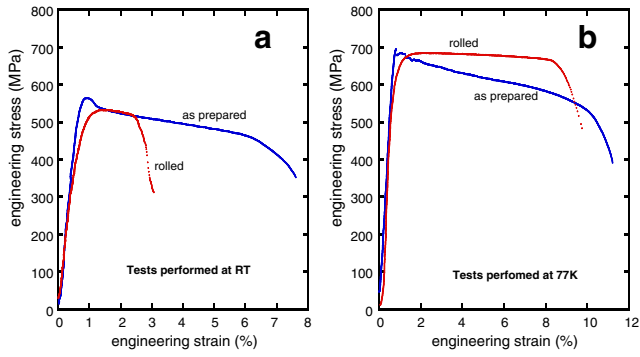


**Figure 3.** Stress–strain curves at a strain rate  $1 \times 10^{-3} \text{ s}^{-1}$  for tensile tests performed for the as-synthesized and rolled material at (a) room temperature and (b) 77 K.

to behave as “expected”, while the as-synthesized sample shows a very clear yield drop. Even after the rolling process the nanoscale twins are believed to be the dominant strengthening mechanism given that the grains are much larger. The strengths of as-synthesized and rolled samples are similar as shown in Figure 3a and b, suggesting the change of the texture is minor in the rolled sample. The strength is enhanced at 77 K for both type of samples (compare Fig. 3a and b), where the number of dislocations that can be activated decreases [17–20]. The lack of yield drop in the rolled material suggests that the initial dislocation density in the samples plays a critical role in determining the yield behavior of nanostructured materials. This could be the reason why the samples processed by severe plastic deformation or ball milling [21,22] do not possess yield peaks. These processes can yield samples with a narrow grain size distribution which act as dislocation barriers; however, the processing also induces large amounts of pre-existing dislocations that prevent the occurrence of yield points. In the case of high nanoscale twin densities UFG copper synthesized by electrodeposition, the lack of a yield point probably arrives from the dislocations induced by grinding the sample from  $\sim 100 \mu\text{m}$  down to 20–30  $\mu\text{m}$  [23,24]. In fact, sample preparation not only affects the yield behavior but also the strength and ductility of nanostructured materials [21]. In our previous publication [16], we also did not observe a yield point, which can be attributed to the overall deformation applied on the thin samples while removing them from the substrate (thickness 25  $\mu\text{m}$ ).

Further analysis of the stress–strain curves presented in Figure 3 reveals that the degree of the yielding peak drop strongly depends on the deformation temperature. We notice in Figure 4 that immediately after the yielding, the yield peak at 77 K plunges much more sharply than it does at room temperature. As the dislocation density is very low at the early stage of the deformation, we suggest that this phenomenon is related to the temperature dependence behavior of the dislocation velocity, which can be expressed as

$$v = f(\sigma)e^{-Q/kT} \quad (1)$$

where  $\sigma$  is the shear stress,  $Q$  is the activation energy for dislocation motion,  $k$  is the Boltzmann constant, and  $T$  is the temperature. Despite the fact that the applied

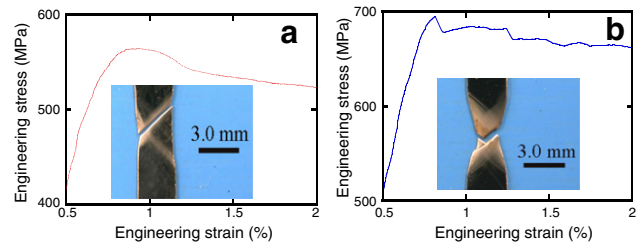


**Figure 4.** Zoom view of the yield peak of the as-prepared samples shown in Figure 3 including optical micrographs of the deformation region at (a) room temperature and (b) 77 K. The deformation of the RT test is mainly confined in a single slip band (inset of (a)) while the deformation at 77 K shows the formation of multiple shear bands which correlates to the flow stress peak oscillation (inset (b)).

stress is higher at 77 K than at room temperature (see Fig. 3), the deformation temperature dictates the dislocation velocity as it is a reciprocal exponential function of the temperature. Consequently, the dislocation velocity ( $v$ ) is lower at liquid nitrogen temperature than at room temperature [1], leading to higher stress levels which have more sharply defined and more densely populated glide bands as can be observed by a much sharper stress drop after the initial yield peak. With the gradual increase of the plastic strain, however, the dislocation annihilation and subsequent recovery are suppressed at 77 K, reducing the dislocation glide distance. This renders a sequence of small yield peaks (Fig. 4b) that are associated with the sudden drops of the flow stress, which eventually become indistinguishable on the stress–strain curve as enough mobile dislocations are accumulated. Interestingly, we observe that the flow stress peak oscillation is correlated with multiple shear bands formed in 77 K deformed samples (inset Fig. 4b). To further verify the presence of the stress peak oscillations we conducted tests at 77 K at various strain rates for which all test showed a large yield peak followed by smaller yield peaks. In contrast, the sharp and multiple flow stress drops are not seen in RT-deformed samples, the stress–strain curves of which are characterized by a single broad yield peak drop, followed by the smooth decrease of the flow stress. Correspondingly, the deformation of all RT-tested samples is mainly confined in a single slip band (shown in the inset of Fig. 4a). The discrepancy of the yield behavior at different temperatures agrees with our view that the yield peak behavior is closely tied to the low dislocation density and nanoscale microstructural characteristics in the current samples.

The yield point of nanostructured materials is of fundamental importance to understand the Hall–Petch strengthening mechanism. Here we have carefully documented the yield behavior of a high-purity, thick ( $\sim 170 \mu\text{m}$ ) nanostructured copper with medium-density nanoscale twins. The observed yield peaks can be associated with the low initial dislocation density of as-fabricated materials and their nanometer scale microstructures. Plastic deformation was observed to be localized to the area of initial deformation band formation indicating very low or zero work hardening. The magnitude of the yield points was insensitive to strain rate but strongly dependent on deformation temperature.

Uniformly distributed mobile dislocations introduced by rolling to 20% reduction in thickness eliminated the yield points at both temperatures investigated. Additionally, uniform deformations greater than 1.5% at room temperature and 7% at liquid nitrogen temperature were introduced by the rolling deformation. These experimental observations clearly demonstrate that the observed yield point behavior is a direct result of the very low initial dislocation density in this sputter-deposited copper foil as expected for “ideal” nanoscale microstructure materials. An approach to enhancing the ductility of such “ideal” nanoscale microstructure materials is also demonstrated by these results. Careful considerations of pre- and post-testing sample characteristics should be exercised in order to understand the true yield behavior of these nanostructured materials.

This work was performed under the auspices of the US Department of Energy by University of California, Lawrence Livermore National Laboratory under Contract W-7405-Eng-48. The authors thank P. Ramsey, E. Sedillo, D. Freeman at LLNL for their assistance in sample preparation, testing and characterization and Dr. Alex Hamza for helpful discussions.

- [1] W.G. Johnston, J.J. Gilman, *J. Appl. Phys.* 30 (1959) 129.
- [2] S. Van Petengem, S. Brandstetter, H. Van Swygenhoven, *Appl. Phys. Lett.* 89 (2006) 073102.
- [3] F. Ebrahimi, L. Hongqi, *J. Mater. Sci.* 42 (2007) 1444.
- [4] L. Hongqi, F. Ebrahimi, *Acta Mater.* 54 (2006) 2877.
- [5] K.S. Kumar, H. Van Swygenhoven, S. Suresh, *Acta Mater.* 51 (2003) 5743.
- [6] M.A. Meyers, A. Mishra, D.J. Benson, *Prog. Mater. Sci.* 51 (2006) 427.
- [7] J. Schiotz, K.W. Jacobsen, *Science* 301 (2003) 1357.
- [8] C.Y. Yu, P.W. Kao, C.P. Chang, *Acta Mater.* 53 (2005) 4019.
- [9] Y.F. Shen, L. Lu, Q.H. Lu, Z.H. Jin, K. Lu, *Scripta Mater.* 52 (2005) 989.
- [10] W.S. Zhao, N.R. Tao, J.Y. Guo, Q.H. Lu, K. Lu, *Scripta Mater.* 53 (2005) 745.
- [11] M. Dao, L. Lu, Y.F. Shen, S. Suresh, *Acta Mater.* 54 (2006) 5421.
- [12] L. Lu, R. Schwaiger, Z.W. Shan, M. Dao, K. Lu, S. Suresh, *Acta Mater.* 53 (2005) 2169.
- [13] T.W. Barbee Jr., In: L. Chang, B.C. Giessen (Eds.), *Synthetic Modulated Structures*, Academic Press, New York, 1985, p. 313.
- [14] T.W. Barbee Jr., *Atomic Engineering with Multilayers*, Lawrence Livermore National Laboratory, December 1997.
- [15] T.W. Barbee Jr., D.L. Keith, in: *Proceedings of the Fall Meeting of the Metallurgical Society AIME*, Pittsburgh, PA, 1980.
- [16] A.M. Hodge, Y.M. Wang, T.W. Barbee Jr., *Mater. Sci. Eng.* 429A (2006) 272.
- [17] H. Conrad, *Mater. Sci. Eng. A – Struct. Mater. Prop. Microstruct. Process.* 341 (2003) 216.
- [18] F. Ebrahimi, G.R. Bourne, M.S. Kelly, T.E. Matthews, *Nanostruct. Mater.* 11 (1999) 343.
- [19] E. Ma, Y.M. Wang, Q.H. Lu, M.L. Sui, L. Lu, K. Lu, *Appl. Phys. Lett.* 85 (2004) 4932.
- [20] Y.M. Wang, E. Ma, *Appl. Phys. Lett.* 85 (2004) 2750.
- [21] S. Cheng, E. Ma, Y.M. Wang, L.J. Keszkes, K.M. Youssef, C.C. Koch, U.P. Trociewitz, K. Han, *Acta Mater.* 53 (2005) 1521.
- [22] Y.M. Wang, E. Ma, *Appl. Phys. Lett.* 83 (2003) 3165.
- [23] L. Lu, L.B. Wang, B.Z. Ding, K. Lu, *J. Mater. Res.* 15 (1999) 270.
- [24] L. Lu, Y. Shen, X. Cheng, L. Qian, K. Lu, *Science* 304 (2004) 422.